Received 3 July 2022; accepted 26 July 2022. Date of publication 11 August 2022; date of current version 22 August 2022.

Digital Object Identifier 10.1109/OJAP.2022.3198287

Enabling High-Fidelity Ultra-Wideband Radio Channel Emulation: Band-Stitching and Digital Predistortion Concepts

YILIN JI AND WEI FAN (Senior Member, IEEE)

Antenna Propagation and Millimeter-Wave Systems Section, Department of Electronic Systems, Aalborg University, 9220 Aalborg, Denmark

CORRESPONDING AUTHOR: W. FAN (e-mail: wfa@es.aau.dk)

This work was supported in part by the Innovation Fund Denmark under Project 1046-0006, and in part by the EURAMET European Partnership on Metrology Programme (MEWS) under the Framework of European COST INTERACT Action under Grant CA20120.

ABSTRACT Channel emulators are the key instrument in radio performance testing. The fidelity of the emulated channel with respect to the target channel models directly affects the credibility of the testing result. In practice, due to some non-idealities of the radio-frequency (RF) components of the emulator, its intrinsic frequency response, i.e., the response of the bypass mode, may not be flat over the frequency band of interest, which leads to an excessive distortion over the target channel models, and hence a less accurate emulated channel. This problem could be even more profound when the emulator engages the band-stitching process for a wider-bandwidth emulation, especially in the transition frequency band between adjacent sub-bands. To enable high-fidelity band-stitched or even ultra-wideband channel emulation, we propose a novel digital pre-distortion concept in this work, where we pre-distort the target channel models according to the measured intrinsic response of the emulator to compensate for its effect on the emulated channel. The proposed method is numerically assessed with measured intrinsic responses of a commercial emulator, and the magnitude and phase variations of the stitched channel reduce by one order of magnitude in comparison to that of the conventional method.

INDEX TERMS Band-stitching, channel emulation, digital pre-distortion, and equalization.

I. INTRODUCTION

IT IS essential to thoroughly evaluate the end-to-end performance of wireless devices under realistic propagation conditions. The concept of virtual drive test (VDT) has attracted great interest [1], [2], [3], [4], where the objective is to bring the conventional field testing to a controllable laboratory environment either with a cable-conducted setup or an over-the-air (OTA) radiated setup [5], [6]. Radio channel emulators are the key component for VDT [7], [8], which physically emulate the radio channel between the transmitter (Tx) and the receiver (Rx). Modern channel emulators are typically designed with a digital architecture due to its high reconfigurability [9], [10], [11], [12], and they have been widely adopted in radio performance testing for various scenarios, e.g., cellular communications, satellite and aerospace non-terrestrial networks (NTN), and wireless local area networks (WLAN).

As new generations of wireless communication technologies emerge, wider and wider radio spectra are allocated to achieve higher data rates. For example, a fifth-generation (5G) new radio (NR) signal can occupy a bandwidth of up to 400 MHz per carrier in the frequency range 2 (i.e., millimeter-wave bands) [13] compared to the fourth-generation (4G) long-term-evolution (LTE) signals taking only 20 MHz bandwidth. It is plausible that an even larger bandwidth or ultra-wideband (UWB) may be used for future generations. However, most currently available commercial channel emulators support an emulation bandwidth of 40 MHz (up to 160 MHz), which poses a limit on testing radios of any larger bandwidth.

To enable UWB channel emulation, a band-stitching technique has been proposed in the literature [14], [15], [16], [17]. In that regime, multiple digital channels of a channel emulator, operating at different intermediate frequencies (IF), are utilized together to synthesize a single virtual digital channel of a larger bandwidth. Ideally, the intrinsic frequency response of each physical digital channel needs to be of raised-cosine, and

the coherence of amplitude and phase between adjacent channels needs to be guaranteed for a perfect band-stitching result. In [15], we briefly showed the effect of a misaligned phase between adjacent channels on the resulting stitched channel, and a huge distortion over the stitched channel was observed.

The coherence misalignment can be resolved by careful emulator calibration to some extent. Currently, emulator calibration for band-stitching has been done mostly in a trial-and-error manner [14], [17], i.e., tuning the attenuation (e.g., at 0.1 dB step) and phase shift (e.g., at 1° step) of each digital channel until the flatness of the frequency response of the stitched channel reaches some acceptable tolerance on a vector network analyzer (VNA). Obviously, even if the whole tuning process is automated, calibration done this way can be very time-consuming and its accuracy is bound to the tuning resolution. Moreover, this calibration method does not account for the shape of the intrinsic frequency response of the digital channels if there is a deviation from the ideal raised-cosine. In a recent work [17], the intrinsic frequency response of a commercial channel emulator was observed to have a magnitude variation of ± 1.5 dB and a phase variation of $\pm 15°$ per digital channel over 160 MHz bandwidth, and the variation worsened to ± 3.5 dB and $\pm 30°$ for the stitched channel of 960 MHz bandwidth with the aforementioned calibration accounted.

For regular cellular-device performance testing, fading channels following, e.g., geometry-based stochastic channel models (GSCM) [18], are typically targeted for emulation. It has been found empirically that the additional intrinsic distortion, on top of the target fading channel, has no or negligible impact on test results. However, for some static-link communication scenarios, e.g., satellite, aerospace, and front/back-haul scenarios, the target channels are expected to be wideband and rather static. Besides, notches may occur in the channel frequency response due to potential strong reflections in the scenarios. It is very popular to test those links with a notch channel model, e.g., the Rummler model [19] or the two-ray model, with variable notch frequencies and depths. In this case, a better emulator calibration method is desired since the notches in the emulated channel would be highly sensitive to the amplitude and phase of the intrinsic frequency response of channel emulators. Another critical scenario could be with error vector magnitude (EVM) measurements, where the intrinsic distortion of emulators needs to be low enough so that it does not obscure the true EVM of devices under test. To the best knowledge of the authors, no solutions have been reported in the literature on mitigating the intrinsic distortion introduced by channel emulators, which can be very important for high-fidelity UWB channel emulation.

In this work, we propose a novel digital pre-distortion scheme for channel emulators to achieve high-fidelity UWB channel emulation. The proposed method is based on the minimum mean square error (MMSE) equalization. By measuring the intrinsic frequency responses of the channel emulator, we can pre-distort the target channel profile accordingly so that the total response of the emulated channel matches the intended target channel with a higher accuracy. This is especially important for the band-stitching process since the proposed method regulates the effective intrinsic responses of the emulator to be the desired raised-cosine, which is a huge advantage against the conventional calibration method. The pre-distorted channel coefficients may result in more taps than the maximum number of taps that are available in a channel emulator. Therefore, we also give a possible solution to derive the pre-distorted channel coefficients under the limitation of the tap resources of channel emulators. The main contribution of the paper is summarized as follows:

- The weakness of the conventional calibration method for band-stitching for channel emulation is discussed.
- A digital pre-distortion scheme as an alternative calibration and fading method is proposed.
- The performance of the proposed method is numerically evaluated with measured intrinsic responses of a commercial channel emulator.
- A possible solution to derive the pre-distorted channel coefficients under the limitation of tap numbers is given.

The rest of the paper is structured as follows: The principle of band-stitching for channel emulation is revisited in Section II. We elaborate the proposed digital pre-distortion scheme for a single digital channel in Section III. Later, the proposed method is applied to a band-stitching scenario and its performance is compared with that of the conventional calibration method in terms of the magnitude and phase variation of the stitched channel. Lastly, Section V concludes the paper.

II. BAND-STITCHING WITH CHANNEL EMULATORS

A. SYSTEM SETUP

Fig. 1 shows a general schematic diagram of stitching two digital channels of a channel emulator into a single virtual digital channel of larger bandwidth for the single-input single-output (SISO) case. It is also scalable to the multiple-input multiple-output (MIMO) case, the diagram of which can be found in [15].

The mixer down-converts the RF input signal x^{RF} to the IF signal x^{IF} with the local oscillator (LO) frequency f_{LO}. The IF signal x^{IF} is split into two identical streams, and each stream is further mixed down to baseband with its individual sub-band center frequency f_1^{IF} and f_2^{IF} respectively. The baseband (BB) signal of each sub-band, x_1^{BB} and x_2^{BB}, is anti-aliasing filtered and then sampled by the analog-to-digital converter (ADC). The discrete baseband signal convolves with the emulated channel, h_1^{BB} and h_2^{BB}, generated according to the target channel model, in the finite impulse response (FIR) filter. The signal of each digital channel is converted to analogue through the digital-to-analog converter (DAC) and up-converted back to its respective IF. The combiner stitches the two streams back to one, which is lastly up-converted to RF to form the RF faded signal y^{RF}

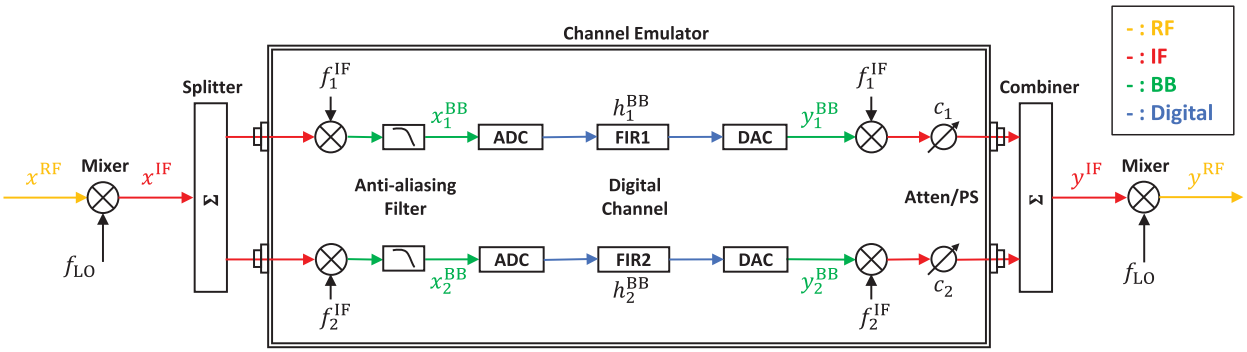

FIGURE 1. Schematic diagram of stitching two sub-bands for a SISO system. Note that the time dependence of the signals is omitted for brevity.

over the stitched band. The variable attenuators and phase shifters (Atten/PS) are used to change the relative amplitude and initial phase, c_1 and c_2, between the two branches for calibration.

B. DIGITAL CHANNEL

The digital channel of each branch can be conceptually simplified and seen as a single FIR filter for ease of understanding as illustrated in Fig. 1. In practice, it typically consists of a set of cascaded FIR filters, namely an input filter, a fading channel filter, and an output filter. The input filter is an all-pass filter with a pre-configured bandwidth relative to the ADC sampling rate, and is used for suppressing potential out-of-band signals for further processing. The fading channel filter is where the target channel for emulation is generated through specifying tap delay indices and associated tap coefficients according to the target channel impulse responses. The output filter is another low-pass filter with a pre-configured bandwidth to further suppress any out-of-band signals before the DAC. Typically, only the fading channel filter is configurable by the users, whereas the other two filters are preset by the emulator vendors and hidden from the users.

The composite baseband impulse response of the ith digital channel, $i \in \{1, 2\}$, can be modelled as

$$h_i^{\mathrm{BB}}(\tau) = h_i^{\mathrm{TRG}}(\tau) * h^{\mathrm{I/O}}(\tau), \tag{1}$$

where $h_i^{\mathrm{TRG}}(\tau)$ and $h^{\mathrm{I/O}}(\tau)$ denote the target channel impulse response and the composite input and output filter response in the delay τ domain, respectively. The notation $*$ denotes convolution.

Given the target channel being an L-delay-tap channel, we can express $h_i^{\mathrm{TRG}}(\tau)$ as

$$h_i^{\mathrm{TRG}}(\tau) = \sum_{l=1}^{L} \alpha_{i,l} \cdot \delta\big(\tau - \tau_{i,l}\big), \tag{2}$$

where $\alpha_{i,l}$ and $\tau_{i,l}$ are the tap coefficient and tap delay index of the lth delay tap, $l \in \{1, \ldots, L\}$, respectively. $\delta(\cdot)$ denotes the Dirac delta function. Note that the sets of $\{\alpha_{i,l}, \tau_{i,l}\}$ are user-configurable as mentioned with the fading channel filter.

C. CONVENTIONAL CALIBRATION METHOD

The total impulse response of the ith branch, from the x^{RF} input port to the y^{RF} output port, can be modelled as

$$h_i^{\mathrm{RF}}(\tau) = h_i^{\mathrm{ANL}}(\tau) * h_i^{\mathrm{BB}}(\tau) \cdot c_i \cdot e^{j2\pi\left(f_{\mathrm{LO}} + f_i^{\mathrm{IF}}\right)\tau}, \tag{3}$$

where $h_i^{\mathrm{ANL}}(\tau)$ denotes the baseband equivalent composite impulse response of the analogue components in the path of the branch, including the mixers, splitter, combiner, and the anti-aliasing filter. The term c_i denotes the complex coefficient of the variable attenuator and phase shifter. The last phase term represents the up-conversion to RF.

For the conventional calibration, the channel emulator is set to the so-called "Bypass" mode, where essentially the same static single-delay-tap channel is emulated in the digital channel of each branch, i.e., $h_i^{\mathrm{BB}}(\tau) = h^{\mathrm{I/O}}(\tau)$. Therefore, $h_i^{\mathrm{RF}}(\tau)$ can be recast for the calibration stage as

$$h_i^{\mathrm{RF,\,cal}}(\tau) = h_i^{\mathrm{ANL}}(\tau) * h^{\mathrm{I/O}}(\tau) \cdot c_i \cdot e^{j2\pi\left(f_{\mathrm{LO}} + f_i^{\mathrm{IF}}\right)\tau}. \tag{4}$$

Let us further denote $h_i^{\mathrm{SYS}}(\tau) = h_i^{\mathrm{ANL}}(\tau) * h^{\mathrm{I/O}}(\tau)$ as the intrinsic impulse response of the ith branch. The total impulse response of the stitched channel can be expressed as a sum of the responses of both branches

$$h^{\mathrm{RF,\,cal}}(\tau) = \sum_i h_i^{\mathrm{SYS}}(\tau) \cdot c_i \cdot e^{j2\pi\left(f_{\mathrm{LO}} + f_i^{\mathrm{IF}}\right)\tau}. \tag{5}$$

Both $h_i^{\mathrm{RF,\,cal}}(\tau)$ and $h^{\mathrm{RF,\,cal}}(\tau)$ can be measured with a VNA in terms of their frequency-domain counterparts, $H_i^{\mathrm{RF,\,cal}}(f)$ and $H^{\mathrm{RF,\,cal}}(f)$ by enabling either one branch at a time or both branches at the same time. The goal of the calibration is to reach a flat or near-flat magnitude frequency response of $H^{\mathrm{RF,\,cal}}(f)$ over the stitched band by tuning the coefficients c_i through the variable attenuator and phase shifter.

D. REQUISITE OF THE INTRINSIC RESPONSE OF EACH BRANCH

For the solution of c_i to exist, a requisite has to be fulfilled, i.e., $h_i^{\mathrm{SYS}}(\tau)$, or its frequency-domain representation $H_i^{\mathrm{SYS}}(f)$, must be of raised-cosine. A raised-cosine filter is specified by two parameters, its 6-dB bandwidth $\frac{1}{T}$ and roll-off factor β $(0 \le \beta \le 1)$ as

$$H^{\mathrm{RC}}(f; T, \beta)$$

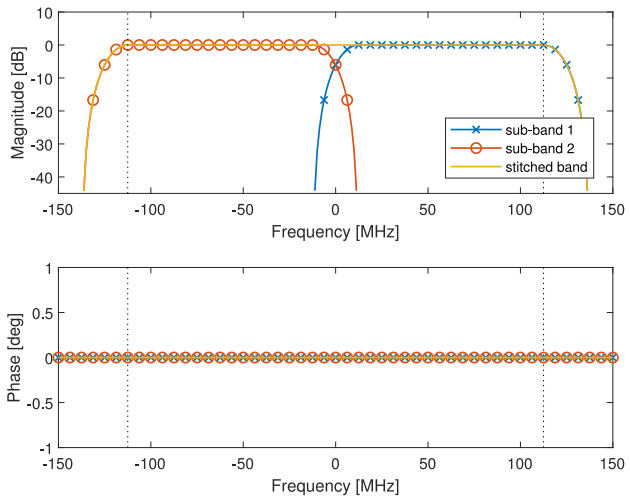

FIGURE 2. (Top) the magnitude and (bottom) the unwrapped phase (normalized at the center frequency) of the frequency response. The black dotted lines indicate the 225 MHz distortion-free bandwidth.

$$= \begin{cases} 1, & |f| \le \frac{1-\beta}{2T} \\ \frac{1}{2}\left(1+\cos\left(\frac{\pi T}{\beta}\left(|f|-\frac{1-\beta}{2T}\right)\right)\right), & \frac{1-\beta}{2T} < |f| \le \frac{1+\beta}{2T} \\ 0, & |f| > \frac{1+\beta}{2T}, \end{cases} \tag{6}$$

which holds odd symmetry about $|f| = \frac{1}{2T}$ in the transition band $\frac{1-\beta}{2T} < |f| \le \frac{1+\beta}{2T}$.

Combining (5) and (6) with $f_i^{\mathrm{IF}} = \pm\frac{1}{2T}$ and $c_i = 1$ for $i \in \{1, 2\}$ respectively, one can find

$$H^{\mathrm{RF,\,cal}}(f) = H^{\mathrm{RC}}\left(f - f_{\mathrm{LO}}; T', \beta'\right), \tag{7}$$

which is also raised-cosine with twice the 6-dB bandwidth ($\frac{1}{T'} = 2\frac{1}{T}$) and half the roll-off factor ($\beta' = \frac{1}{2}\beta$) centered at f_{LO}. The resulting intrinsic distortion-free (flat) bandwidth of the stitched band is $B = (2-\beta)\frac{1}{T}$ which is about twice as large as that of a single branch, $(1-\beta)\frac{1}{T}$, given a small value of β. Note that a smaller β requires a larger number of taps to implement in an FIR filter, which may more likely exceed the maximum number of taps available in the fading channel filter as further discussed in Section III-C.

Fig. 2 shows an example of an ideal $H_i^{\mathrm{RF,\,cal}}(f)$ and $H^{\mathrm{RF,\,cal}}(f)$, with $\frac{1}{T} = 125$ MHz and $\beta = 0.2$. The resulting intrinsic distortion-free bandwidth is $B = 225$ MHz. Note that the raised-cosine in (6) is zero-phase. For a causal system, the phase response will be slanted instead of zero-phase.

III. DIGITAL PRE-DISTORTION—AN ALTERNATIVE CALIBRATION AND FADING METHOD

A. EQUALIZATION WITH FADING CHANNEL FILTER

In the conventional calibration method, the only degree of freedom of users is tuning the variable attenuator and phase shifter of each branch. If the measured branch response $H_i^{\mathrm{RF,\,cal}}(f)$, or essentially, $H_i^{\mathrm{SYS}}(f)$, deviates from the desired

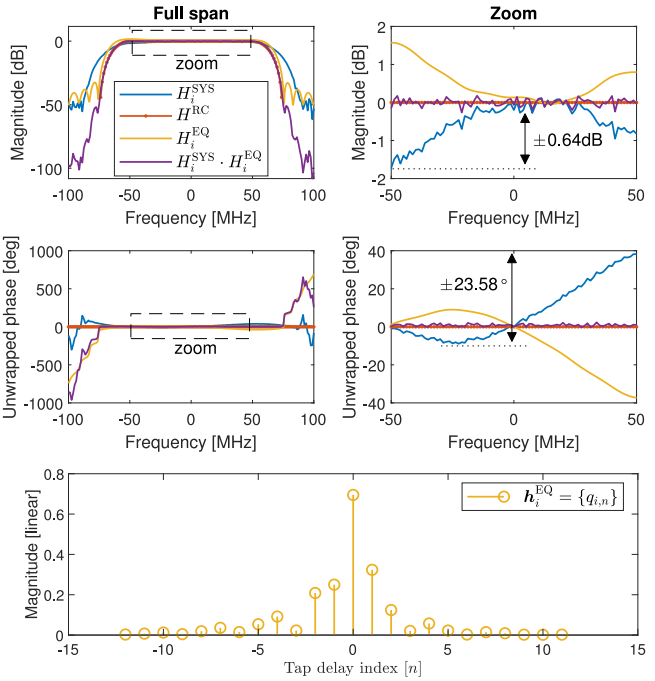

FIGURE 3. An example of the equalization for a measured system response $H_i^{\mathrm{SYS}}(f)$ of a commercial channel emulator. $H^{\mathrm{RC}}(f; T, \beta)$ denotes the target raised-cosine, $H_i^{\mathrm{EQ}}(f)$ denotes the frequency response of the equalization filter, and $H_i^{\mathrm{SYS}}(f) \cdot H_i^{\mathrm{EQ}}(f)$ denotes the effective intrinsic system response after the equalization. h_i^{EQ} denotes the vector of the tap coefficients of the equalization filter.

raised-cosine, just tuning branch coefficients c_i will not correct it. However, this can be done with the aforementioned fading channel filter, which is typically the only filter in the emulator that the users have access to.

In this case, the calibration problem can be formulated to an equalization problem: We want to find the coefficients of an N-tap equalization filter $\boldsymbol{h}_i^{\mathrm{EQ}} = \{q_{i,n}\} \in \mathbb{C}^{N\times 1}$, $n \in \{1, \ldots, N\}$, whose frequency response $H_i^{\mathrm{EQ}}(f)$ satisfies

$$H_i^{\mathrm{SYS}}(f) \cdot H_i^{\mathrm{EQ}}(f) \approx H^{\mathrm{RC}}(f; T, \beta), \tag{8}$$

where $\approx$ denotes approximate. Given the measured $H_i^{\mathrm{SYS}}(f)$ and the target $H^{\mathrm{RC}}(f; T, \beta)$, $H_i^{\mathrm{EQ}}(f)$ can be solved with the minimum mean square error (MMSE) method as

$$H_i^{\mathrm{EQ}}(f) = \frac{\left\{H_i^{\mathrm{SYS}}(f)\right\}^{\dagger} \cdot H^{\mathrm{RC}}(f; T, \beta)}{|H_i^{\mathrm{SYS}}(f)|^2 + \sigma^2(f)},$$
$$\sigma^2(f) = \frac{\sigma_n^2(f)}{\left|H^{\mathrm{RC}}(f; T, \beta)\right|^2}, \tag{9}$$

where $\{\cdot\}^{\dagger}$ denotes complex conjugate, and $\sigma_n^2(f)$ is the power spectral density of the noise, which can be estimated from the noise floor of the measurement. The coefficients of $\boldsymbol{h}_i^{\mathrm{EQ}}$ can be calculated through the inverse discrete Fourier transform (IDFT) of $H_i^{\mathrm{EQ}}(f)$ over the N tap delays.

A numerical example of the equalization is illustrated in Fig. 3, which includes the magnitude and phase of

the frequency response of a measured $H_i^{\mathrm{SYS}}(f)$, a target $H^{\mathrm{RC}}(f;T,\beta)$, the resultant $H_i^{\mathrm{EQ}}(f)$, and the product $H_i^{\mathrm{SYS}}(f)\cdot H_i^{\mathrm{EQ}}(f)$. A 24-tap equalization filter is considered in this example, and the resultant tap coefficients are shown at the bottom of Fig. 3. The system response $H_i^{\mathrm{SYS}}(f)$ was measured for a commercial channel emulator (Propsim F8). The clock rate of the digital channel was 200 MHz (i.e., 5 ns tap delay interval). The parameters of the raised-cosine were set to $\frac{1}{T}=125$ MHz and $\beta=0.2$. The settings correspond to a distortion-free bandwidth of 100 MHz, which is denoted as "Zoom".

Across this bandwidth, there is a ± 0.64 dB magnitude variation and $\pm 23.58°$ phase variation before the equalization, and the variations are significantly reduced after the equalization to ± 0.25 dB and $\pm 1.28°$, respectively. Note that there exists a much larger deviation between the $H_i^{\mathrm{SYS}}(f)$ and the $H^{\mathrm{RC}}(f;T,\beta)$ in the transition frequency band as can be seen in the magnitude response under "Full span", which is not reflected by the variation metrics given above. Those large deviations in the transition band violate the odd symmetry for the band-stitching process, and lead to a deteriorated intrinsic frequency response of the stitched channel as shown later in Section IV.

B. PRE-DISTORT TARGET CHANNEL WITH EQUALIZATION COEFFICIENTS

To utilize the fading channel filter for both the equalization purpose and the target channel emulation (its original purpose), one can convolve the coefficients of the target channel with the obtained equalization coefficients, and set that to be the new target channel to emulate in the fading channel filter. This is referred to as the digital pre-distortion (DP) process. The impulse response of the new target channel can be expressed as

$$h_i^{\mathrm{DP}}(\tau)=h_i^{\mathrm{TRG}}(\tau)*h_i^{\mathrm{EQ}}(\tau), \tag{10}$$

$$h_i^{\mathrm{EQ}}(\tau)=\sum_{n=1}^{N} q_{i,n}\cdot\delta(\tau-\tau_n), \tag{11}$$

where τ_n is the nth tap delay of the equalization filter. One can form the coefficients and tap delay of $h_i^{\mathrm{DP}}(\tau)$ as two vectors, $\boldsymbol{h}_i^{\mathrm{DP}}=\{w_{i,m}\}\in\mathbb{C}^{M\times 1}$ and $\boldsymbol{\tau}_i^{\mathrm{DP}}=\{\tau_{i,m}\}\in\mathbb{C}^{M\times 1}$ with M being the resultant number of taps of $h_i^{\mathrm{DP}}(\tau)$, and load them to the fading channel filter to realize equalization and fading simultaneously.

A numerical example of the pre-distortion is illustrated in Fig. 4, which includes the magnitude and phase of the frequency response of a band-unlimited target channel, $H_i^{\mathrm{TRG}}(f)$, the emulated channel without pre-distortion, $H_i^{\mathrm{SYS}}(f)\cdot H_i^{\mathrm{TRG}}(f)$, and that with pre-distortion, $H_i^{\mathrm{SYS}}(f)\cdot H_i^{\mathrm{DP}}(f)$. The target channel is set to be a two-ray channel with a delay difference of 3 tap intervals, i.e., 15 ns, and a power ratio of 3 dB between the two rays, as shown at the bottom of Fig. 4. Across the 100 MHz distortion-free bandwidth, there is a large deviation for the case without

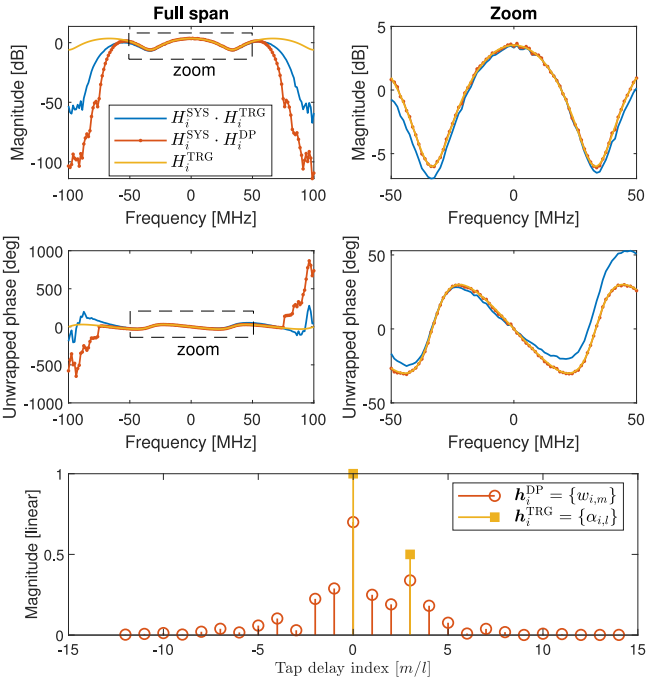

FIGURE 4. An example of the pre-distortion for a target channel $H_i^{\mathrm{TRG}}(f)$ with the resultant pre-distorted channel coefficients. $H_i^{\mathrm{SYS}}(f)\cdot H_i^{\mathrm{TRG}}(f)$ denotes the emulated channel without the pre-distortion, and $H_i^{\mathrm{SYS}}(f)\cdot H_i^{\mathrm{DP}}(f)$ denotes the emulated channel with the pre-distortion. h_i^{TRG} denotes the vector of the tap coefficients of the original target channel, and h_i^{DP} denotes that of the fading channel filter with the pre-distortion method.

pre-distortion with respect to the target channel in terms of both magnitude and phase, whereas negligible deviation for the case with pre-distortion.

C. TAP RESOURCES OF FADING CHANNEL FILTER

Different commercial channel emulators have different maximum numbers of available taps, $\tilde{M}$, in the fading channel filter. For example, the Spirent Vertex channel emulator has up to 24 taps [7] and the Keysight Propsim channel emulator has up to 48 taps [8]. The length of the resultant pre-distorted channel coefficients $\boldsymbol{h}_i^{\mathrm{DP}}$ needs to be no greater than that number, i.e., $M\le\tilde{M}$.

In the case of the example given in Fig. 4, the resultant $\boldsymbol{h}_i^{\mathrm{DP}}$ requires 27 taps, which could be larger than the maximum number of available taps for a specific channel emulator. In this case, one can use the same equalization method given in Section III-A by changing the equalization target from $H^{\mathrm{RC}}(f;T,\beta)$ to $H^{\mathrm{RC}}(f;T,\beta)\cdot H_i^{\mathrm{TRG}}(f)$. The pre-distortion coefficients can be obtained in a similar way as (9) as

$$\tilde{H}_i^{\mathrm{PD}}(f)=\frac{\{H_i^{\mathrm{SYS}}(f)\}^{\dagger}\cdot H^{\mathrm{RC}}(f;T,\beta)\cdot H_i^{\mathrm{TRG}}(f)}{|H_i^{\mathrm{SYS}}(f)|^2+\tilde{\sigma}^2(f)},$$

$$\tilde{\sigma}^2(f)=\frac{\sigma_n^2(f)}{|H^{\mathrm{RC}}(f;T,\beta)\cdot H_i^{\mathrm{TRG}}(f)|^2}, \tag{12}$$

and the coefficients $\tilde{\boldsymbol{h}}_i^{\mathrm{DP}}=\{\tilde{w}_{i,\tilde{m}}\}\in\mathbb{C}^{\tilde{M}\times 1}$ can be calculated through the IDFT over the $\tilde{M}$ tap delay $\tilde{\boldsymbol{\tau}}_i^{\mathrm{DP}}=\{\tilde{\tau}_{i,\tilde{m}}\}\in\mathbb{C}^{\tilde{M}\times 1}$.

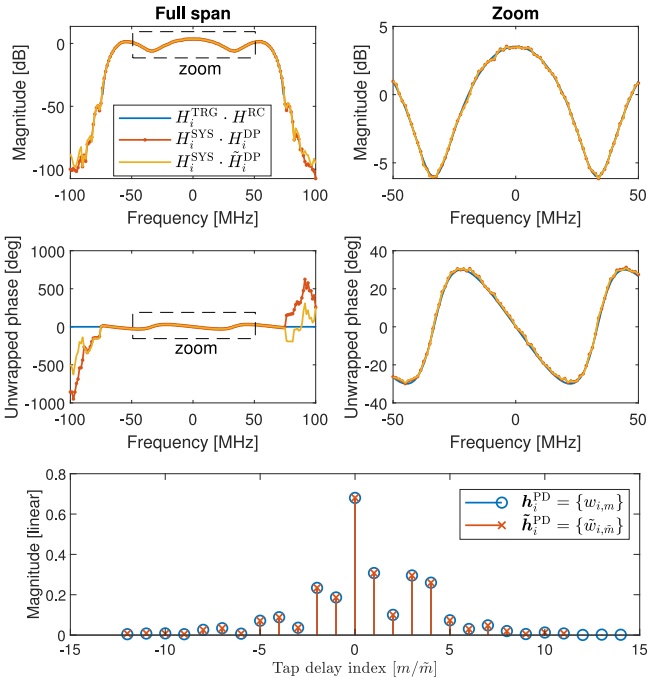

FIGURE 5. An example of the pre-distortion for a target channel $H^{\mathrm{RC}}(f; T, \beta) \cdot H_i^{\mathrm{TRG}}(f)$ with the resultant pre-distorted channel coefficients. $H_i^{\mathrm{SYS}}(f) \cdot H_i^{\mathrm{DP}}(f)$ denotes the emulated channel with the 27-tap pre-distortion coefficients $\boldsymbol{h}_i^{\mathrm{DP}}$, and $H_i^{\mathrm{SYS}}(f) \cdot \tilde{H}_i^{\mathrm{DP}}(f)$ denotes that with the shortened 24-tap pre-distortion coefficients $\tilde{\boldsymbol{h}}_i^{\mathrm{DP}}$.

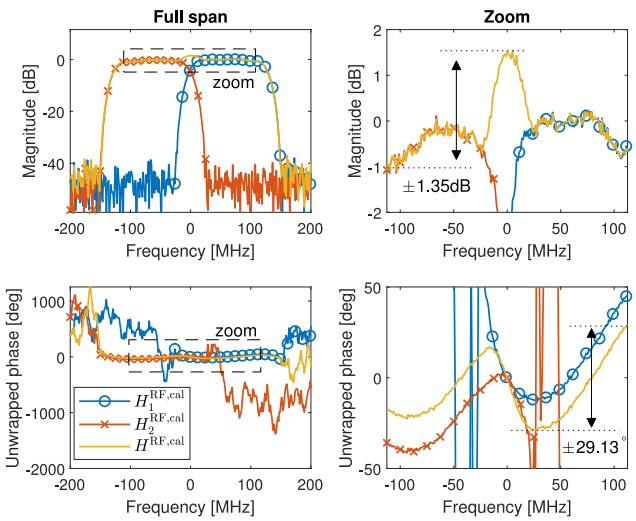

FIGURE 6. The measured intrinsic responses $H_i^{\mathrm{RF,\,cal}}(f)$ and $H^{\mathrm{RF,\,cal}}(f)$ of a channel emulator for band-stitching with the conventional calibration method. $H_1^{\mathrm{RF,\,cal}}(f)$ and $H_2^{\mathrm{RF,\,cal}}(f)$ denote the frequency responses of the higher and lower sub-bands, respectively. $H^{\mathrm{RF,\,cal}}(f)$ denotes the frequency response of the stitched channel.

An example is shown in Fig. 5, where the length of the pre-distorted channel coefficients, $\tilde{\boldsymbol{h}}_i^{\mathrm{DP}}$, is limited to 24, i.e., 3 taps fewer than that of $\boldsymbol{h}_i^{\mathrm{DP}}$. The deviations in the frequency response with the $\tilde{\boldsymbol{h}}_i^{\mathrm{DP}}$ case increase to ±0.27 dB for magnitude and ±1.71° for phase compared to that with the $\boldsymbol{h}_i^{\mathrm{DP}}$ case, i.e., ±0.25 dB and ±1.28°.

IV. DIGITAL PRE-DISTORTION FOR BAND-STITCHING

We consider stitching two digital channels of a channel emulator (Propsim F8) into a signal virtual digital channel of a larger bandwidth operating at the center frequency of 28 GHz. The raised-cosine with parameters $\frac{1}{T} = 125$ MHz and $\beta = 0.2$ is targeted for each branch, which corresponds to a 225 MHz distortion-free bandwidth for the stitched channel.

The system setup is the same as in Fig. 1. An LO frequency of 33.1 GHz is generated with an analogue signal generator, which results in an IF frequency of 5.1 GHz after the external mixer. Following the design rule of the band-stitching given in Section II-D, the center frequencies of the two branches are set to $f_1^{\mathrm{IF}} = 5.1625$ GHz and $f_2^{\mathrm{IF}} = 5.0375$ GHz respectively so that $|f_1^{\mathrm{IF}} - f_2^{\mathrm{IF}}| = \frac{1}{T}$. The intrinsic frequency response of each branch, i.e., $H_1^{\mathrm{RF,\,cal}}(f)$ and $H_2^{\mathrm{RF,\,cal}}(f)$, are measured with a VNA from 27.5 GHz to 28.5 GHz with 801 frequency samples.

Fig. 6 shows the magnitude and phase frequency response of the stitched channel from the conventional method. The center 400 MHz band of the measurement is denoted as "Full span", and the center 225 MHz band of the measurement, i.e., the targeted distortion-free band of the stitched channel, is denoted as "Zoom". Across the distortion-free band, there is a ±1.35 dB magnitude variation and ±29.13° phase variation for the stitched channel. Compared to the single band case as in Fig. 3, the increased variations are caused mostly by the intrinsic response of each branch in the transition band being different from the targeted raised-cosine.

Applying the equalization process introduced in Section III-A to both branches regulates the intrinsic response of each branch to the targeted raised-cosine, and the equalized intrinsic response of each branch and the resultant stitched channel are shown in Fig. 7. Both the magnitude and phase variations are significantly reduced to ±0.26 dB and ±1.34°, respectively, which are both one order of magnitude smaller than that of the conventional method. The equalization coefficients for both branches are shown at the bottom of Fig. 7.

Furthermore, the target two-ray channel is pre-distorted with the respective equalization coefficients of each branch to emulate the target channel in the band-stitched virtual digital channel of 225 MHz bandwidth. The resultant frequency responses of the emulated channel with the conventional calibration method and with the digital pre-distortion method are shown in Fig. 8. The band-unlimited frequency response of the target two-ray channel is also shown alongside as a reference. The result from the pre-distortion method clearly outperforms that from the conventional method in terms of both magnitude and phase deviations.

The pre-distorted coefficients $\boldsymbol{h}_1^{\mathrm{DP}}$ and $\boldsymbol{h}_2^{\mathrm{DP}}$ for the two branches are shown at the bottom of Fig. 8. By loading $\{\boldsymbol{h}_1^{\mathrm{DP}}, \boldsymbol{\tau}_1^{\mathrm{DP}}\}$ and $\{\boldsymbol{h}_2^{\mathrm{DP}}, \boldsymbol{\tau}_2^{\mathrm{DP}}\}$ to the corresponding fading channel filters of a channel emulator, the considered two-ray

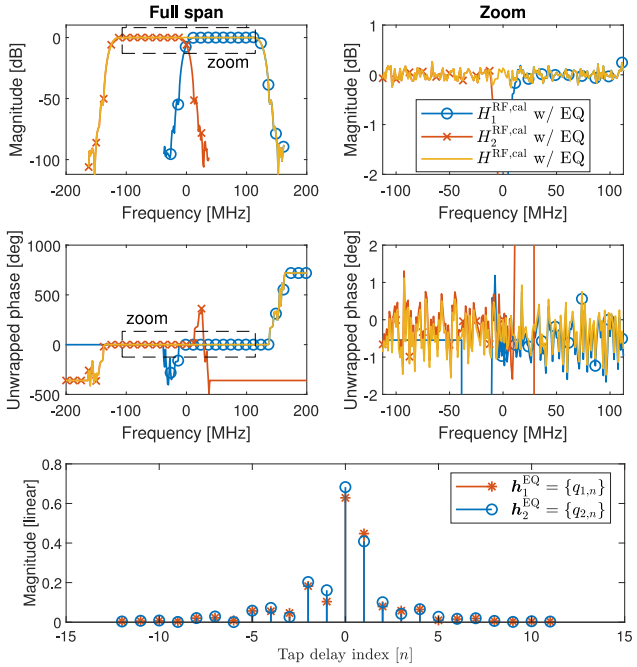

FIGURE 7. The equalized intrinsic frequency responses $H_i^{\mathrm{RF,\,cal}}(f)$ and $H^{\mathrm{RF,\,cal}}(f)$ of a channel emulator for band-stitching with the equalization method. $H_1^{\mathrm{RF,\,cal}}(f)$ and $H_2^{\mathrm{RF,\,cal}}(f)$ denote the frequency responses of the upper and lower sub-bands, respectively. $H^{\mathrm{RF,\,cal}}(f)$ denotes the frequency response of the stitched channel.

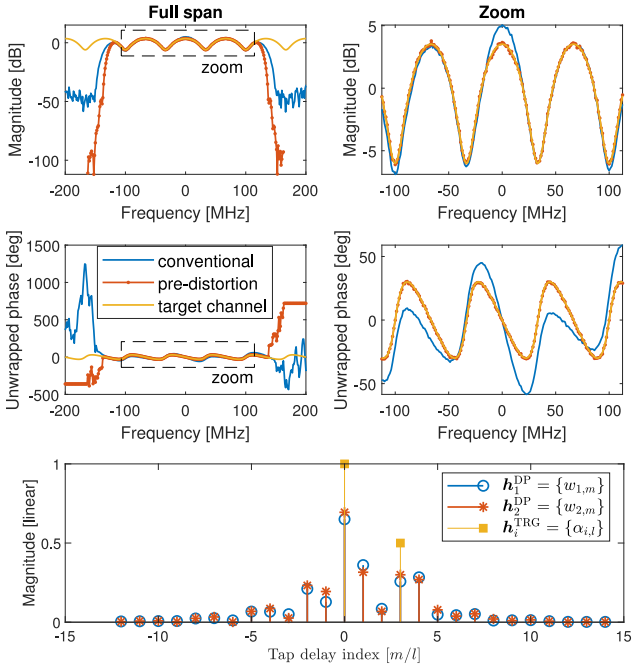

FIGURE 8. The frequency responses of the emulated channel over the stitched band with the conventional calibration method and the digital pre-distortion method. $\boldsymbol{h}_i^{\mathrm{TRG}}$ denotes the vector of the tap coefficients of the original target channel, and $\boldsymbol{h}_1^{\mathrm{DP}}$ and $\boldsymbol{h}_2^{\mathrm{DP}}$ denote the vector of the tap coefficients of the fading channel filter with the pre-distortion method for the upper and lower sub-bands, respectively.

channel can be emulated with high fidelity over a roughly doubled bandwidth. The same principle can be extended for band-stitching with more digital channels, and high-fidelity ultra-wideband emulation can be realized.

V. CONCLUSION

In this paper, we revisited the conventional calibration method for the band-stitching for ultra-wideband channel emulation. To overcome its weakness at reshaping the intrinsic response of each sub-band to raised-cosine, we proposed a digital pre-distortion method, which exploited the user-accessible fading channel filter in the channel emulator. The proposed method can be thought of as the convolution between the original target fading channel and an equalization filter, where the raised-cosine is set as the equalization target. The coefficients of the equalization filter were solved with the minimum mean square error method.

The proposed method costs extra number of taps of the fading channel filter, which is a limited resource of a channel emulator. To confine the number of taps of the resultant pre-distorted channel coefficients, the original target fading channel and the raised-cosine were considered as a whole as the equalization target, and the equalization coefficients were calculated over the confined taps. The resultant equalization coefficients correspond directly to the final pre-distorted channel coefficients.

Both the proposed method and the conventional method were numerically assessed with the measured intrinsic responses of a commercial channel emulator for a two-band stitching scenario. The linearity of the intrinsic response of the stitched channel, i.e., the variations of the magnitude and phase, were used as the figure of merit for the band-stitching performance. It was observed that the variations of the magnitude and phase were ± 1.35 dB and $\pm 29.13°$ with the conventional method and ± 0.26 dB and $\pm 1.34°$ with the proposed method, where both the magnitude and the phase variation were reduced by one order of magnitude.

ACKNOWLEDGMENT

The authors would like to thank the technical discussion with Dr. Pekka Kyösti with Oulu University and Keysight technologies, Finland.

REFERENCES

[1] (Keysight Technol., Santa Rosa, CA, USA). *S8709A Virtual Drive Test Toolset*. [Online]. Available: https://www.keysight.com/us/en/product/S8709A/s8709a-5g-virtual-drive-test-toolset.html

[2] L. C. Jager, P. Berlt, C. Bornkessel, and M. A. Hein, "Distributed spatial channel emulation for virtual drive testing based on multiple software-defined radios," in *Proc. 13th Eur. Conf. Antennas Propag.*, 2019, pp. 1–5.

[3] M. Charitos *et al.*, "LTE-A virtual drive testing for vehicular environments," in *Proc. IEEE Veh. Technol. Conf.*, 2017, pp. 1–5.

[4] Y. Ji *et al.*, "Virtual drive testing over-the-air for vehicular communications," *IEEE Trans. Veh. Technol.*, vol. 69, no. 2, pp. 1203–1213, Feb. 2020.

[5] M. Rumney, "Testing 5G: Time to throw away the cables," *Microw. J.*, vol. 59, no. 11, pp. 10–18, 2016.

[6] T. Eichler, U. Philipp, H. Mellein, and L. Rädler, "Virtual cable calibration for OTA testing of 5G mmWave devices," *Microw. J.*, vol. 64, no. 5, pp. 1–5, 2021.
[7] "Spirent vertex channel emulator," Data Sheet, Spirent, Crawley, U.K. [Online]. Available: https://www.spirent.com/assets/u/spirent_vertex_channel_emulator_datasheet
[8] "Propsim F8 channel emulator," Data Sheet, Keysight Technol., Santa Rosa, CA, USA, 2016.
[9] J. J. Olmos, G. Antoni, F. J. Casadevall, and G. Femenias, "Design and implementation of a wide-band real-time mobile channel emulator," *IEEE Trans. Veh. Technol.*, vol. 48, no. 3, pp. 746–764, May 1999.
[10] N. Zhang, G. Yang, and J. Zhai, "A low complexity emulation scheme for 5G millimeter-wave massive MIMO channel," *Microw. Opt. Technol. Lett.*, vol. 59, no. 6, pp. 1300–1305, 2017.
[11] A. Schwind, P. Berlt, M. Lorenz, C. Schneider, and M. A. Hein, "Implementation of a MIMO channel emulator for over-the-air LTE testing using software defined radio," in *Proc. German Microw. Conf.*, 2018, pp. 307–310.
[12] M. Hofer *et al.*, "Real-time geometry-based wireless channel emulation," *IEEE Trans. Veh. Technol.*, vol. 68, no. 2, pp. 1631–1645, Feb. 2019.
[13] *NR; User Equipment (UE) radio transmission and reception; Part 2: Range 2 Standalone, V17.1.0*, 3GPP Standard TS 38.101-2, 2021.
[14] W. Fan, P. Kyösti, L. Hentilä, and G. F. Pedersen, "A flexible millimeter-wave radio channel emulator design with experimental validations," *IEEE Trans. Antennas Propag.*, vol. 66, no. 11, pp. 6446–6451, Nov. 2018.
[15] Y. Ji, W. Fan, and G. F. Pedersen, "Wideband radio channel emulation using band-stitching schemes," in *Proc. 14th Eur. Conf. Antennas Propag. (EuCAP)*, 2020, pp. 1–5.
[16] J. Cao, F. Tila, and A. Nix, "Wideband RF channel emulation platform for 5G mmWave systems," in *Proc. 2nd IEEE Middle East North Africa Commun. Conf. (MENACOMM)*, 2019, pp. 5–9.
[17] J. Cao, F. Tila, and A. Nix, "Design and implementation of a wideband channel emulation platform for 5G mmWave vehicular communication," *IET Commun.*, vol. 14, no. 14, pp. 2369–2376, 2020.
[18] *Study on Channel Model for Frequencies From 0.5 to 100 GHz*, 3GPP Standard TR 138 901, 2020.
[19] W. Rummler, "A new selective fading model: Application to propagation data," *Bell Syst. Tech. J.*, vol. 58, no. 5, pp. 1037–1071, Jun. 1979.

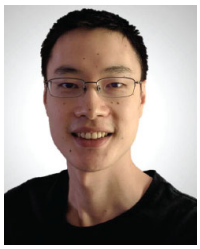

YILIN JI received the B.Sc. degree in electronics science and technology and the M.Eng. degree in integrated circuit engineering from Tongji University, China, in 2013 and 2016, respectively, and the Ph.D. degree in wireless communications from Aalborg University, Denmark, in 2021, where he is currently a Postdoctoral Fellow with the Antennas, Propagation and Millimeter-wave Systems Section. His main research areas are propagation channel characterization, and MIMO over-the-air testing.

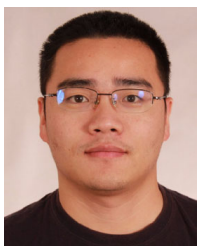

WEI FAN (Senior Member, IEEE) received the Bachelor of Engineering degree from the Harbin Institute of Technology, China, in 2009, the master's double degree (with Highest Hons.) from the Politecnico di Torino, Italy, and Grenoble Institute of Technology, France, in 2011, and the Ph.D. degree from Aalborg University, Denmark, in 2014. From February 2011 to August 2011, he was with Intel Mobile Communications, Denmark, as a Research Intern. He conducted a three-month internship with Anite Telecoms Oy, Finland, in 2014. He is currently an Associate Professor with the Antennas, Propagation and Millimeter-wave Systems Section, Aalborg University. His main areas of research are over-the-air testing of multiple-antenna systems, radio channel sounding, modelling, and emulation.